CHANNEL CROSS-SECTIONS AND INVERSIONS IN HADRIACUS CAVI, MARS AND IMPLICATIONS FOR FORMATIONAL ENVIRONMENT. M. L. Barton, J. A. Skinner, Jr., and C. M. Fortezzo. Astrogeology Science Center, U. S. Geological Survey, 2255 N. Gemini Drive, Flagstaff, AZ, 86001 (mbarton@usgs.gov).

Introduction: Hadriacus Cavi are irregularly-shaped depressions located south of Hadriacus Palus and west of Terby crater along the northeast rim of Hellas basin. The cavi, which expose a sequence of ~500 m-thick stratified rocks, are located between, and post-date topographic promontories interpreted to be associated with the Hellas basin-forming impact (4.0 to 4.1 Ga [1]). Hadriacus Cavi strata provide a glimpse into the range and interaction of geologic processes that immediately followed the Hellas impact including local volcanism, fluvial erosion of the adjacent highland terrains, and collective transport and deposition into massif-bounded structural basins.

Recent large-scale (1:24,000) geologic mapping of cavi-related strata reveals a series of predominantly conformable, massive to stratified, varying light- to dark-toned rock units that exhibit a range of geomorphic textures [1-2], suggesting an active and perhaps rapidly-changing depositional history during the Noachian [2]. We have mapped the full sequence of strata into four main rock groups based on stratigraphic position, lateral continuity, and the presence of unique geologic features [3]. From oldest to youngest, these are (1) the dark-toned, mostly massive, slope-forming "basal" group (80-180 m thick), (2) the light- and dark-toned, mostly stratified, cliff-forming "cavi" group (60-80 m thick), (3) the light-toned, mostly massive, slope- and cliff-forming "mons" group (120-150 m thick), and (4) the light- and dark-toned, massive to stratified, slope-forming "palus" group (80-140 m thick). Here, we present detailed characteristics of a 12 to 15 meter thick, light-toned, channel-bearing subunit of the "cavi" group (**Fig. 1**), which conformably overlies a columnar-jointed subunit interpreted as lava flows and (or) welded volcaniclastics [1].

Methods and Data: Our 1:24,000-scale geologic mapping is based on a 1.5 m/px DTM and associated 0.5 m/px orthoimages created from HiRISE stereo-pair ESP_031924_1525 / ESP_032069_1525 (created via SOCET Set using methods of [4]). During mapping efforts, we noted occurrences of flat-topped, lens-like features that appeared confined to a particular, relatively thin stratigraphic horizon, which we interpret as channel cross-sections. To better understand the vertical and lateral extent of these features and their implied depositional environment, we traced the top and bottom of each cross-section using ArcGIS and calculated max/min elevation statistics by intersecting a 0.5 m-buffer around each line with the HiRISE DTM. The cross-section top provided an estimate of apparent (not actual) channel widths (**Fig. 2**). Channel depths were calculated by subtracting the max and min elevation. We corroborated GIS-derived calculations with spot measurements for all mapped channel cross-sections. We then estimated the plane of occurrence of these channels by creating a triangular irregular network (TIN) using the midpoint of the traced surface line of each mapped channel cross-section (**Fig. 1A**).

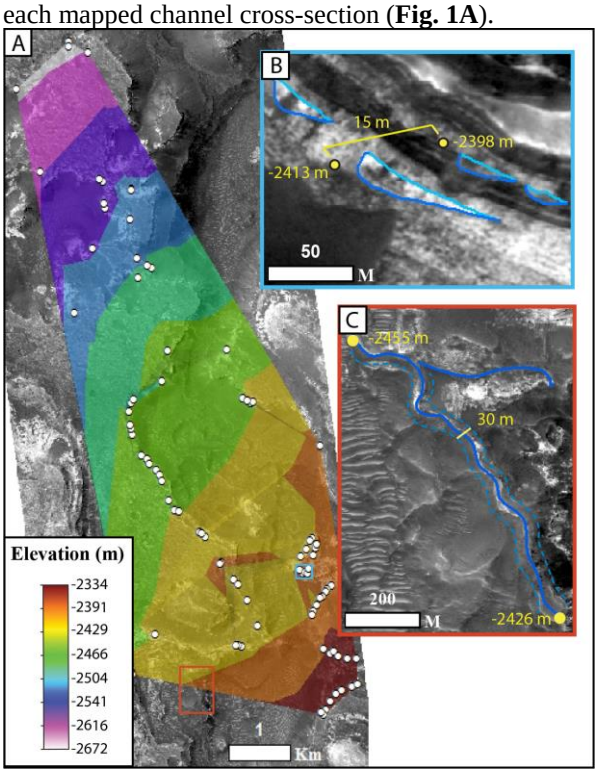

Figure 1. Characteristics of the Hadriacus Cavi channels. (A) Study area showing locations of mapped channel cross-sections (white dots) and the resulting paleo-surface of channel-bearing subunit in the "cavi" group. Surface dips to NNW by 1.7°, equivalent to orientations of bounding units [2]. (B) Example channel cross-sections. Note both the stacked and lateral occurrence of the channels and the light-dark pattern of the outcrop. Subunit thickness here is ~15 m. Inset location indicated by blue box in panel A. (C) Inverted, sinuous channel with surface slope of 1.8° to the NNW, equivalent to the mapped channel cross-sections. Dashed lines indicate the apparent width of the channel, and the solid line represents a basic outline of the channel shape. Inset location indicated by red box in panel A.

Results: We identify 96 unique channel cross-sections in the Hadriacus Cavi study region, which occur over an area of ~36 km^2. The channel cross-sections are generally lighter toned than the surrounding unit (**Fig. 1B**) and are identifiable based on this contrast. The channel bases are predominately single features that are either symmetric or asymmetric. The bases are mostly concave-up with some planar examples. The channel tops are predominately planar with some examples having a very slight convex-up appearance. We specifically note that the calculated widths are apparent rather than actual due to a lack of knowledge of how they transect the original channel; the minimum calculated values are likely to be more representative of the actual channel widths. Schematic depictions of the channels as well as their inferred channel locations are shown in **Fig. 2**. Channel depths range from 0.4 to 13.7 m (mean of 4.2 m ± std dev of 2.7 m) and apparent widths range from 10.4 to 201.9 m (57.9 ± 36.4 m). All channels occur within an elevational range of -2672 to -2334 m (-2447 ± 74 m).

The TIN generated from channel cross-section locations forms a near-planar surface that dips to the NNW by 1.7° (polynomial fits to the same points provide equivalent surfaces). These ridges are 8-12 m wide, 4-6 m tall, and >1 km long and have a sinuosity of 1.13. These features occur from -2426 to -2455 m elevation (**Fig. 1**), within an equivalent range of elevations for the channel-bearing subunit.

Interpretation: Hadriacus Cavi occurs in intermediate-elevation terrain located between high-standing massifs to the SE and the (relatively) low-lying Hadriacus Palus to north. We suggest that the channel cross-sections define a paleo-surface that is equivalent to the orientation of the mapped cavi strata (~2º to the NNW), indicating that the channels were synformational to the bulk of the mapped cavi strata and formed by flow away from the higher-standing massifs located immediately to the south and toward an inferred depocenter, the uppermost surface of which is currently represented by the surface of Hadriacus Palus. Moreover, the sinuous ridges we identify exist at equivalent orientations and stratigraphic horizons, implying these are likely channel inversions. As such, we postulate that we have documented a paleo-channel system in three dimensions. Based on the relatively small size of these cross-sectional lenses, and the low-lying topographic slope of the channel bearing unit, it is possible that these channels are part of a distributary system, though we acknowledge observational limitations that complicate definitive assessment of fluvial environments. There is no immediate evidence of a large-watershed during the formation of these channels. Conformable contacts between these subjacent units imply rapid deposition of volcanic material and the immediately subsequent modification by fluvial processes.

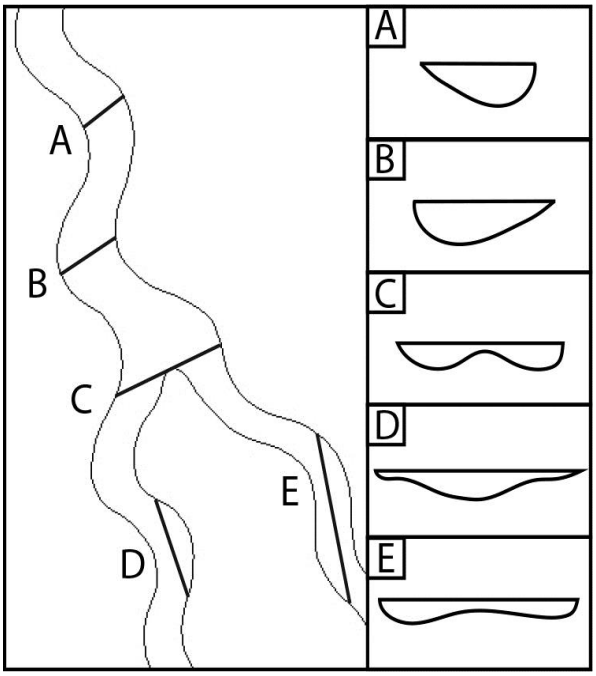

Figure 2. Schematic of the relationship between the observed channel cross-sections the interpreted plan view of a channel system that could produce these shapes.

Based on the measurements and channel morphologies mentioned above, we interpret the Hadriacus Cavi channels as part of a local distributary fluvial system. Although there are known limitations to this interpretation, when compared to a terrestrial channel classification model, we see similarities between the channel system implied by the cross-sections and inverted ridge and terrestrial channels that are found in distributary systems [5]. The low sinuosity value of the inverted channels imply that the system is comprised of multiple, smaller channels rather than a large meandering system. If these channels belong to a distributary system, it implies that there was a larger basin into which these channels debouched, presumably located immediately to the north beneath the current palus surface.

Acknowledgements: This work was funded by NASA PG&G award #NN12AU831I (PI Skinner).

References: [1] Skinner, J. A., Jr. et al. (2015) *LPS XLVII*, Abstract #2806. [2] Skinner, J. A., Jr. et al. (2017) *LPS XLVIII*, Abstract #2694. [3] Barton, M. L. et al. (2017) *LPS XLVIII*, Abstract #2290. [4] Kirk, R. L, et al. (2009) *LPS XL*, Abstract #1414. [5] Gibling, M. R (2006) *Journal of Sedimentary Research*, v. 76, 731-770.